UDC 551.513.1:551.510.522

Parameterization of the Planetary Boundary Layer for Use in General Circulation Models[1]

JAMES W. DEARDORFF—*National Center for Atmospheric Research,[2] Boulder, Colo.*

ABSTRACT—The surface stress and fluxes of heat and moisture are parameterized for use in numerical models of the general circulation of the atmosphere. The parameterization is designed to be consistent with recent advances in knowledge of both the planetary boundary layer and the surface layer. A key quantity throughout is the height, h, of the planetary boundary layer, which appears in the governing stability parameter, a bulk Richardson number. With upward heat flux, a time-dependent prediction equation is proposed for h that incorporates penetrative convection and vertical motion. Under stable conditions, h is assumed to depart from the neutral value and to become nearly proportional to the Monin-Obukhov length.

The roughness length, z_0, is incorporated in the combination h/z_0, and the parameterization is consistent with h/z_0 affecting only the wind component in the direction of the surface velocity. The direction of the surface wind and stress is derived in a manner consistent with the known value of the surface pressure gradient and theoretical studies of the decrease of stress with height.

The parameterization has been tested numerically and appears to be efficient enough to use in existing general circulation models.

1. INTRODUCTION

The planetary boundary layer (PBL) is the region adjacent to the earth's surface where small-scale turbulence is induced by wind shear and/or thermal convection and occurs almost continuously in space and time. It includes in its lowermost portion the Prandtl or surface layer, where the vertical fluxes of heat, momentum, and moisture have nearly the same magnitudes as they do at the surface itself. By contrast with the PBL, turbulence on the subsynoptic scale occurs only intermittently in the rest of the troposphere. Above the PBL, the mechanisms which cause turbulent transport are towering cumulus clouds, clear-air turbulence associated with internal wind shear layers, and effects of topography on a scale large enough to cause upward propagation of energy through the PBL.

A general circulation model (GCM) of the earth's atmosphere should treat the PBL in a physically realistic way to relate the turbulent fluxes at the surface to the calculated variables from the GCM. Two approaches seem possible. One is to place several layers (perhaps five or six) within the lowest 2–3 km above the surface to resolve the vertical structure of the PBL crudely but explicitly. Even in this case, however, the associated vertical transports of heat, momentum, and moisture should be parameterized in a manner consistent with the existence of a PBL within the layers.

The second approach is to parameterize all aspects of the PBL in a GCM that has such poor vertical resolution that the top of the PBL may sometimes not even reach the level of the lowest interior gridpoints. The first approach may be preferable but is usually not feasible, especially with the ever present desire to increase the horizontal resolution of any model. The second approach has not been seriously attempted mainly because of lack of knowledge about properties of the PBL. However, this knowledge is beginning to accumulate, as may be seen from recent studies by Csanady (1967), Blackadar and Tennekes (1968), Gill (1968), Deardorff (1970*a*, 1970*b*), Clarke (1970*a*, 1970*b*), Tennekes (1970), Lenschow (1970), Lettau and Dabberdt (1970), and others. It therefore seems appropriate to attempt a parameterization of the properties of the PBL at this time, using the second approach. The symbols used are identified in table 1.

The basic procedure to be followed here involves splitting the problem into four parts:

1. Use the existing height, h, of the top of the PBL above sea level and values at the lowest one or two grid levels of the GCM to obtain estimates of the vertically averaged mean values of wind velocity, potential temperature, and specific humidity within the PBL.

2. Estimate the surface fluxes of momentum, heat, and moisture using a bulk Richardson number based upon differences between mean values obtained above in step 1 and the surface values. This estimate makes use of our knowledge of both the surface layer and the entire PBL.

3. Estimate the direction of the surface-level velocity using the known value of the horizontal pressure gradient at the surface. This step makes use of PBL theory and the results of step 2 and is necessary so that the direction of the surface stress can be known. The mean wind speed occuring in the bulk Richardson number can then be refined to become the component in the direction of the surface wind and steps 2 and 3 can be repeated if necessary.

[1] The research reported in this paper was done mainly at the University of California, Los Angeles, and supported in part by National Science Foundation Grant No. GA-22756.

[2] Sponsored by the National Science Foundation

4. Obtain $h(X, Y, t+\Delta t)$, given $h(X, Y, t)$, by means of a prognostic equation in unstable cases and a simpler relationship in stable cases. Here, X and Y are the eastward and northward pointing directions, respectively, and Δt is the time step of the GCM. This step utilizes GCM velocities and the surface fluxes obtained from step 2 or its iteration.

TABLE 1.—*Symbols used in this paper*

c	a constant relating the pressure gradient along x to $u_*^2/(\bar{h}-\bar{z}_s)$
c_1	a constant in the eddy-coefficient formulation
C_u	friction coefficient u_*/u_m
C_θ	heat-transfer coefficient
f	magnitude of the Coriolis parameter
F	functional dependence of inverse friction coefficient upon $\bar{h}/z_0$ and $\bar{h}/L$
g	gravitational acceleration
G	functional dependence of inverse heat-transfer coefficient upon $\bar{h}/z_0$ and $\bar{h}/L$
GCM	general circulation model of the atmosphere
h	height above mean sea level of the top of the PBL (subscript also)
k	Kármán constant=0.35
K	eddy coefficient in prognostic equation for $\bar{h}$
L	Monin-Obukhov length
p	pressure obtained from the GCM (subscript also)
PBL	planetary boundary layer
q	specific humidity
r_C	cloud-cover ratio at $z=\bar{h}$
R	constant=0.74 occurring in surface-layer temperature-profile formulation
Ri_B	bulk Richardson number
Ri_C	critical value of Ri_B
S	penetrative convection term in prediction equation for $\bar{h}$
t	time
u	velocity component in x direction
u_*	friction velocity based upon surface stress
$\overline{u'w'}$	x-component of vertical momentum flux, normalized by density
U	velocity component in X direction
v	velocity component in y direction
V	velocity component in Y direction
$\mathbf{V}$	total velocity vector
w	vertical velocity component in general
w_*	convective velocity scale based upon surface heat flux and z_i and g/θ_{vm}
$\overline{w'q'}$	moisture flux
$\overline{w'\theta'}$	kinematic sensible heat flux
W	vertical velocity from GCM
W_C	average cumulus updraft speed at $z=\bar{h}$
W_{ho}	W at $z=\bar{h}$ in regions outside of towering cumuli
x	coordinate in direction of mean wind close to the surface (subscript also)
X	eastward pointing coordinate (subscript also)
y	horizontal coordinate orthogonal to x
Y	northward pointing coordinate (subscript also)
z	vertical coordinate (positive upward)
$\hat{z}$	height above surface scaled by $h-z_s$
z_0	roughness length
$\bar{(\ )}$	overbar: horizontal average over GCM grid area
$(\ )'$	prime: local deviation from a centered grid-area average

Subscripts (not defined above)

1	lowest interior level of GCM where U, V, θ, q are calculated
2	the level $\frac{1}{2}\Delta z$ higher where W is calculated
3	the level $\frac{1}{2}\Delta z$ higher where U, V, θ, q are again calculated, etc.
a	"anemometer" level, taken to be 0.025 $(\bar{h}-\bar{z}_s)$
i	evaluation at inversion base (unstable case)
m	mean value within PBL
N	neutral-stability value
r	relative value
s	surface value
v	virtual (potential temperature)

Greek symbols

β	constant=4.7
γ	constant=15
γ''	constant=9
γ_θ	an average rate of increase of $\bar{\theta}$ with height
ΔX, ΔY	grid increments of the GCM
$\Delta\theta_i$	potential temperature jump at $z=z_i$
ζ	stability variable: $\log_{10}(-\mathrm{Ri}_B)-3.5$
η	stability variable in diabatic profile for temperature
θ	potential temperature
κ	thermal diffusivity of air
υ	kinematic viscosity of air
ξ	stability variable in diabatic profile for wind
ρ	air density
σ	standard deviation (in the horizontal)
τ	wind stress
ψ	angle measured counterclockwise from X-axis
∇	gradient operator
∇_H	horizontal gradient operator

These four steps are treated separately in sections 2–5. Section 6 treats the vertical distribution of fluxes within the PBL when its height exceeds the height of interior grid levels of the GCM. In section 7, the results of preliminary tests of this parameterization are presented.

2. MEAN VALUE WITHIN THE PBL

A grid value located in the lowest interior level of a GCM, at level z_1, say, actually represents the average of the variable from the surface, z_s, to a height of about $2(z_1-z_s)$ above z_s. It is considered to be averaged horisontally over the grid area also, and an overbar will designate the grid-area average. If $\bar{h}-\bar{z}_s$, which is believed to be 1 km typically, happens to equal $2(z_1-\bar{z}_s)$, then the grid value U_1, for example, exactly equals the mean value U_m within the PBL. See figure 1 for the numbering of the grid levels. The vertical resolution of a GCM is sometimes such that this condition is approximated. In that case, variables stored at the lowest interior GCM level provide an excellent starting point in the procedure to obtain the surface fluxes. The following mean variables are needed: eastward and northward velocity components, U_m and V_m, the potential temperature, θ_m, and the specific humidity, q_m.

Generally, however, $\bar{h}$ will lie considerably above or below the GCM level of $z_2=2(z_1-\bar{z}_s)+\bar{z}_s$ (see fig. 1). Then any number of procedures may be used to estimate U_m, V_m, θ_m, and q_m, knowing $\bar{h}$. The one suggested here

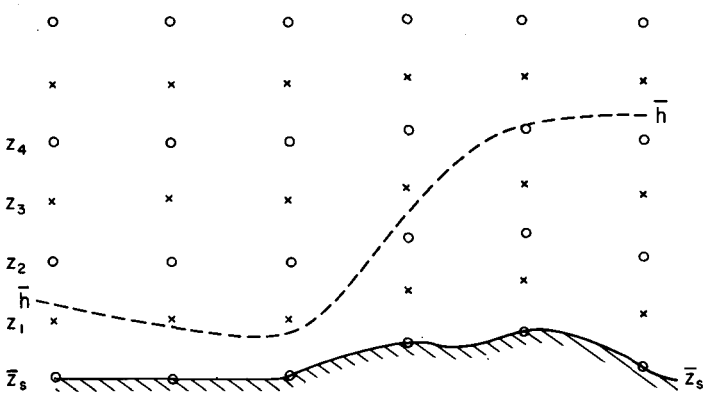

FIGURE 1.—Schematic representation of the surface, $\bar{z}_s$, the height, $\bar{h}$, of the planetary boundary layer, and GCM grid levels, $z_1, \ldots, z_4$. The xs denote grid points at which U, V, θ, and q are calculated; the os denote points where W is calculated.

for its simplicity is to extrapolate from levels 1 and 3 within the GCM to the mid-PBL level of $\frac{1}{2}(\bar{h}+\bar{z}_s)$; that is,

$$U_m=U_1+(U_3-U_1)\left(\frac{\bar{h}+\bar{z}_s}{2}-z_1\right)/(z_3-z_1) \qquad (1)$$

and similarly for V_m, θ_m, and q_m. Thus, if $\frac{1}{2}(\bar{h}+\bar{z}_s)$ should equal z_1 or z_2, U_m is given by U_1 or $\frac{1}{2}(U_1+U_3)$, respectively, without need of extrapolation or interpolation. [Revision of eq (1) is necessary if the grid levels do not follow the topography as in fig. 1.] If $\bar{h}$ exceeds z_4, eq (1) may still be applied, with $\frac{1}{2}(\bar{h}+\bar{z}_s)$ replaced by z_2, because the PBL is then apt to be well mixed.

The above method is least satisfactory when the PBL is shallow and capped by a very strong temperature inversion. To treat such circumstances with some rigor, one might instead utilize time-dependent equations for θ_m and q_m (and possibly U_m and V_m) in addition to the prognostic equations already in use within the GCM at interior grid levels. This would add the term $[(\bar{\theta}_h-\theta_m)d\bar{h}/dt]/(\bar{h}-\bar{z}_s)$ to the right-hand side of a prognostic equation for θ_m, for example. Although the added terms involving $d\bar{h}/dt$ are available, $\bar{\theta}_h$ and $\bar{q}_h$ would be relatively uncertain quantities for which evaluation might in turn require new prognostic equations. Because of this and other complications, the second method is beyond the scope of this paper but has been discussed by Lilly (1968).

3. ESTIMATE OF SURFACE FLUXES WITH UNKNOWN SURFACE FLOW DIRECTION

Surface-layer formulations relate the surface fluxes of sensible heat and moisture to the vertical gradients of $\bar{\theta}$ and $\bar{q}$, respectively, at anemometer level, z_a, and to the friction velocity, $u_*=(\tau_s/\rho_s)^{1/2}$. Here, τ_s is the surface stress, which is assumed directed in the downstream, x, direction near the surface, ρ is density, and the subscript s refers to evaluation at the surface. The surface layer is defined to be sufficiently shallow that the vertical flux of a quantity at z_a is little different than at z_s.

To extend surface-layer formulations far into the PBL, we must make use of PBL studies in which, again, the velocity along the surface flow direction is an important factor. We will then need to make use of u_m, where u is the velocity component in the x-direction, whereas only the mean velocity $\mathbf{V}_m(X, Y, t)$ is immediately available from the GCM using eq (1). The directions of $\mathbf{V}_m$ and u_m generally differ by 10° or more, depending upon effects of thermal stability, height of the PBL, baroclinicity, and vertical resolution of the GCM. At this early stage in the solution for the surface fluxes, it will be assumed that u_m approximately equals $|\mathbf{V}_m|$. The surface stress obtained with the aid of this assumption can be utilized to estimate the difference between the flow direction of the mean PBL and that existing at height $\bar{z}_a$. If the difference is enough to cause u_m^2 to be significantly smaller than $\mathbf{V}_m^2$, the revised value for u_m may be utilized in a manner described later to obtain improved estimates of the surface fluxes. Subsequently, a revised surface flow direction may be obtained.

Treatment of the Surface Layer

In this layer, the dimensionless vertical gradients of wind, temperature, and specific humidity are believed to be functions of $(z-\bar{z}_s)/L$ only, where L is the Monin-Obukhov length given by

$$L=-u_*^3\Big/\left[k\frac{g}{\theta_{vm}}(\overline{w'\theta_v'})_a\right]. \qquad (2)$$

Here, k is Kármán's constant, g is the gravitational acceleration, and θ_v is the virtual potential temperature. The kinematic vertical flux of *virtual* potential temperature, $\overline{w'\theta_v'}$, is used here since this quantity appears in the turbulence kinetic energy equation as a source or sink if the density perturbations associated with moisture fluctuations are taken into account in a Boussinesq approximation. The kinematic vertical flux is related to the sensible heat and moisture fluxes by

$$(\overline{w'\theta_v'})_a\approx(\overline{w'\theta'})_a+0.61\theta_m(\overline{w'q'})_a. \qquad (3)$$

The primes refer to local deviations from the GCM grid-area average. The thermal stability of the PBL will be designated as

$$\left.\begin{aligned}&\text{unstable if } (\overline{w'\theta_v'})_a>0 \quad \text{with } (\theta_{vs}-\theta_{vm})>0\\&\text{neutral if } (\overline{w'\theta_v'})_a=0 \quad \text{with } (\theta_{vs}-\theta_{vm})=0\\&\text{stable if } (\overline{w'\theta_v'})_a<0 \quad \text{with } (\theta_{vs}-\theta_{vm})<0.\end{aligned}\right\} \qquad (4)$$

It will become apparent later that the methods used to obtain the surface fluxes ensure that $(\overline{w'\theta_v'})_a$ has the same sign as $\bar{\theta}_{vs}-\theta_{vm}$.

It is assumed that the surface values $\bar{\theta}_s$ and $\bar{q}_s$ are known, either from climatological evaluation for use over the sea or from calculations based upon the surface thermal energy balance. The quantity $\bar{\theta}_{vs}$ is given approximately by

$$\bar{\theta}_{vs}=\bar{\theta}_s(1+0.61\bar{q}_s) \qquad (5)$$

and similarly for subscript m replacing s.

The formulations by Businger et al. (1971), that revise the earlier ones by Businger (1966), will be used here because, for the first time, a large number of direct measurements were taken of both heat flux and momentum flux under both stable and unstable conditions. Their formulation for the neutral or unstable case is

$$\left(\frac{kz_r}{u_*}\right)\frac{\partial \bar{u}}{\partial z}=\left(1-\frac{\gamma z_r}{L}\right)^{-1/4} \tag{6}$$

and

$$\left[\frac{kz_r u_*}{(-\overline{w'\theta_v'})_a}\right]\frac{\partial \bar{\theta}_v}{\partial z}=R\left(1-\frac{\gamma'' z_r}{L}\right)^{-1/2} \tag{7}$$

and in the stable case is

$$\left(\frac{kz_r}{u_*}\right)\frac{\partial \bar{u}}{\partial z}=1+\frac{\beta z_r}{L} \tag{8}$$

and

$$\left[\frac{kz_r u_*}{(-\overline{w'\theta_v'})_a}\right]\frac{\partial \bar{\theta}_v}{\partial z}=R+\frac{\beta z_r}{L}. \tag{9}$$

Here, z_r is the relative height, $\bar{z}_a-\bar{z}_s$, and the constants are given by $\gamma=15$, $\gamma''=9$, $R=0.74$, $\beta=4.7$, and $k=0.35$. The smaller value than 0.40 for k is thought to be an effect of the much larger Reynolds number in the lower atmosphere relative to that in a wind tunnel. The value of 0.74 for R instead of unity is another novel result and reflects the observation of Businger et al. (1971) that the ratio of the eddy diffusivity for heat to that for momentum [the ratio of eq (6) to (7), or eq (8) to (9)] approaches about $1.35=R^{-1}$ for neutral or stable stratification. The study by Webb (1970) also indicates that this ratio of eddy diffusivities remains near unity in stable conditions rather than becoming much less than unity. One sees in eq (9) that the temperature measurements of Businger et al. (1971) have been applied to $\bar{\theta}_r$, and not just to $\bar{\theta}$. The justification lies in the identity between the eddy coefficients for sensible heat and moisture found by Dyer (1967).

A practical advantage of eq (6) and (7) over the competing (KEYPS) formulation (Panofsky 1963) is its direct integrability in terms of familiar functions. It has been shown by Paulson (1970) that the integrals of eq (6) and (7) from z_0 to z_r are

$$\frac{\bar{u}_a}{u_*}=\frac{1}{k}\left\{\log_e\left(\frac{z_r}{z_0}\right)-\left[\log_e\left(\frac{1+\xi^2}{2}\right)+2\log_e\left(\frac{1+\xi}{2}\right)-2\tan^{-1}\xi+\frac{\pi}{2}\right]\right\} \tag{10}$$

and

$$\frac{(\bar{\theta}_{va}-\bar{\theta}_{vs})u_*}{(-\overline{w'\theta_v'})_a}=\frac{R}{k}\left[\log_e\left(\frac{z_r}{z_0}\right)-2\log_e\left(\frac{1+\eta^2}{2}\right)\right] \tag{11}$$

in the unstable or neutral case, where

$$\xi=\left(1-\frac{\gamma z_r}{L}\right)^{1/4} \tag{12a}$$

and

$$\eta=\left(1-\frac{\gamma'' z_r}{L}\right)^{1/4} \tag{12b}$$

In the stable case, the integration of eq (8) and (9) gives the familiar log-linear profiles

$$\frac{\bar{u}_a}{u_*}=\frac{1}{k}\left[\log_e\left(\frac{z_r}{z_0}\right)+\frac{\beta z_r}{L}\right] \tag{13}$$

and

$$\frac{(\bar{\theta}_{va}-\bar{\theta}_{vs})u_*}{(-\overline{w'\theta_v'})_a}=\frac{R}{k}\left[\log_e\left(\frac{z_r}{z_0}\right)+\frac{\beta}{R}\frac{z_r}{L}\right]. \tag{14}$$

It is assumed in the derivations of eq (11) and (14) that the roughness length, z_0, which is the increment above the surface at which the downward extrapolated property equals its surface equilibrium value, is the same for $\bar{u}$ and $\bar{\theta}_v$. There is evidence that this is approximately true over water from measurements by Fleagle et al. (1958) and by Hasse (1968). However, little or no evidence is available for land surfaces. It is also assumed that computer storage is available within the GCM for z_0 values appropriate to land surfaces averaged over large scale. The values suggested by Fiedler et al. (1971) for most land surfaces range from 20 to 70 cm. For the sea surface, a constant value of z_0 between 0.02 and 0.03 cm gives the value for the drag coefficient obtained directly by Miyake et al. (1970).

Next, the differences in $\bar{u}$ and $\bar{\theta}_v$ across the bulk of the PBL above the surface layer will be treated so that the surface fluxes of momentum and heat can be related to u_m and $\bar{\theta}_{vs}-\theta_{vm}$.

Treatment of the PBL Above the Surface Layer

In this part of the PBL, properly defined dimensionless velocity and temperature *deficits* are believed to be functions of $(\bar{h}-\bar{z}_s)/L$ and independent of $(\bar{h}-\bar{z}_s)/z_0$. In the unstable case, $\bar{h}$ is here considered to be identical with the height of the inversion base, z_i, capping the PBL (Lilly 1968, Deardorff 1970*b*), while in the neutral or stable case $\bar{h}$ is generally deemed proportional to u_*/f where f is the magnitude of the Coriolis parameter (Clarke 1970*a*). It should be remarked, however, that some investigators (e.g., Clarke 1970*a*, Tennekes 1970) hold that the height of the unstable momentum boundary layer may still be proportional to u_*/f even when the height of the thermal boundary layer is z_i.

For neutral and unstable cases, the data obtained numerically by Deardorff (1970*a*, 1970*b*, 1972) will be utilized. There the level $\bar{z}_a$ was chosen to be

$$\bar{z}_a=\bar{z}_s+0.025(\bar{h}-\bar{z}_s) \tag{15}$$

which seems sufficiently small to satisfy the surface-layer requirement of nearly constant flux between $z=\bar{z}_s$ and $\bar{z}_a$. The same relation will thus be used here. Dimensionless profiles of $\bar{u}$ and $\bar{\theta}_v-\bar{\theta}_{vs}$, averaged over an ensemble of realizations, were subsequently averaged vertically throughout the PBL and compared with values at $\bar{z}_a$. Three different stabilities were initially treated: $-(\bar{h}-\bar{z}_s)/L=0$, 4.5, and 45. The main results of interest here are given in table 2. (Most of each deficit listed in the table occurred in the lower portion of the PBL, and at

TABLE 2.—*Comparison of profiles of* $\bar{u}$ *and* $\bar{\theta}_v-\bar{\theta}_{vs}$ *averaged vertically throughout the* PBL *and compared with values at* $\bar{z}_a$

$-(\bar{h}-\bar{z}_s)/L$	$(u_m-\bar{u}_a)/u_*$	$(\theta_{vm}-\bar{\theta}_{va})u_*/(-\overline{w'\theta'_v})_a$
0.0	8.43	7.30 (limiting case)
1.5	4.40	3.17
4.5	2.54	1.59
45.5	1.53	0.55

higher levels small positive values of $\partial\bar{\theta}/\partial z$, with countergradient heat flux, actually occurred.) From these values, the following interpolation formulas were obtained:

$$\left.\begin{aligned}\frac{u_m-\bar{u}_a}{u_*}&=8.4\left[1-\frac{50(\bar{h}-\bar{z}_s)}{L}\right]^{-0.16} \qquad (16)\\ \text{and}\qquad \frac{u_*(\theta_{vm}-\bar{\theta}_{va})}{(-w'\theta'_v)_a}&=7.3\left[1-\frac{5.8(\bar{h}-\bar{z}_s)}{L}\right]^{-0.47} \qquad (17)\end{aligned}\right\}(w'\theta'_v)_a>0.$$

Although the constant factor within the brackets of eq (16) is nearly 10 times larger than that of eq (17), the larger negative exponent in eq (17) reflects the finding of table 2 that, for significant thermal instability, the potential temperature deficit is more easily wiped out by convective mixing than is the momentum deficit.

In the stable case, Clarke's (1970*a*) observations for $u_*/(fL)=210$ will be utilized except that the different stability parameter, $(\bar{h}-\bar{z}_s)/L$, will be used here. This procedure should be no less correct if $\bar{h}$ is known from other considerations; it also has the advantage of yielding finite stability at the Equator. From Clarke's observations, it is estimated that $(\bar{h}-\bar{z}_s)$ was about $0.23u_*/f$ if in neutral cases the top of the PBL is judged to lie at $0.35u_*/f$. It then follows that $(\bar{h}-\bar{z}_s)/L\approx 48$ for Clarke's stable case. Due to the absence of observations at other average degrees of thermal stability, it will be assumed simply that the functional dependence of the deficits is linear in $(\bar{h}-\bar{z}_s)/L$. Then table 2 for neutral stability and Clarke's profiles for the stable case suggest that

$$\left.\begin{aligned}\frac{u_m-\bar{u}_a}{u_*}&=8.4+\frac{0.6(\bar{h}-\bar{z}_s)}{L} \qquad (18)\\ \text{and}\qquad \frac{(\theta_{vm}-\bar{\theta}_{va})u_*}{(-w'\theta'_v)_a}&=7.3+\frac{0.6(\bar{h}-\bar{z}_s)}{L} \qquad (19)\end{aligned}\right\}(\overline{w'\theta'_v})_a<0.$$

The factor 0.6 is, unfortunately, uncertain by at least ±30 percent even if the linear stability dependence is essentially correct.

Combination of Surface-Layer and PBL-Deficit Formulations

The surface-layer formulations [eq (10)–(14)] may be combined with the PBL-deficit formulations [eq (16)–(19)] using also eq (15) and the definition $z_r=\bar{z}_a-\bar{z}_s$, by elimination of $\bar{u}_a$ and $\bar{\theta}_{va}$. The result in the neutral and unstable case is

$$\frac{u_m}{u_*}\equiv\frac{(u_m-\bar{u}_a)}{u_*}+\frac{\bar{u}_a}{u_*}=\frac{1}{k}\left\{\log_e\left[\frac{0.025(\bar{h}-\bar{z}_s)}{z_0}\right]-\log_e\left(\frac{1+\xi^2}{2}\right)-2\log_e\left(\frac{1+\xi}{2}\right)+2\tan^{-1}\xi-\frac{\pi}{2}\right\}+8.4\left[1-\frac{50(\bar{h}-\bar{z}_s)}{L}\right]^{-0.16}=F\left[\frac{(\bar{h}-\bar{z}_s)}{z_0},\frac{(\bar{h}-\bar{z}_s)}{L}\right] \qquad (20)$$

and

$$\frac{(\theta_{vm}-\bar{\theta}_{vs})u_*}{(-\overline{w'\theta'_v})_a}=\frac{R}{k}\left\{\log_e\left[\frac{0.025(\bar{h}-\bar{z}_s)}{z_0}\right]-2\log_e\left(\frac{1+\eta^2}{2}\right)\right\}+7.3\left[1-\frac{5.8(\bar{h}-\bar{z}_s)}{L}\right]^{-0.47}=G\left[\frac{(\bar{h}-\bar{z}_s)}{z_0},\frac{(\bar{h}-\bar{z}_s)}{L}\right] \qquad (21)$$

where

$$\xi=\left[1-\frac{0.025\gamma(\bar{h}-\bar{z}_s)}{L}\right]^{1/4} \qquad (22a)$$

and

$$\eta=\left[1-\frac{0.025\gamma''(\bar{h}-\bar{z}_s)}{L}\right]^{1/4}. \qquad (22b)$$

In the stable case, the result is

$$\frac{u_m}{u_*}=\frac{1}{k}\log_e\left[\frac{0.025(\bar{h}-\bar{z}_s)}{z_0}\right]+8.4+\frac{0.93(\bar{h}-\bar{z}_s)}{L}=F\left[\frac{(\bar{h}-\bar{z}_s)}{z_0},\frac{(\bar{h}-\bar{z}_s)}{L}\right] \qquad (23)$$

and

$$\frac{(\theta_{vm}-\bar{\theta}_{vs})u_*}{(-\overline{w'\theta'_v})_a}=\frac{R}{k}\log_e\left[\frac{0.025(\bar{h}-\bar{z}_s)}{z_0}\right]+7.3+\frac{0.93(\bar{h}-\bar{z}_s)}{L}=G\left[\frac{(\bar{h}-\bar{z}_s)}{z_0},\frac{(\bar{h}-\bar{z}_s)}{L}\right]. \qquad (24)$$

In both cases, we see that the right-hand sides are functions only of $(\bar{h}-\bar{z}_s)/z_0$ and of $(\bar{h}-\bar{z}_s)/L$.

Now, if eq (21) or (24) is multiplied by $(g/\theta_{vm})(\bar{h}-\bar{z}_s)$ and divided by the square of eq (20) or (23), respectively, we find that

$$\frac{\frac{g}{\theta_{vm}}(\bar{h}-z_s)(\theta_{vm}-\bar{\theta}_{vs})}{u_m^2}\equiv \mathrm{Ri_B}=\frac{1}{k}\left(\frac{\bar{h}-\bar{z}_s}{L}\right)\frac{G}{F^2} \qquad (25)$$

where $\mathrm{Ri_B}$ is a bulk Richardson number. Because of the existence of eq (25), the problem may be inverted and solved numerically in advance to yield the friction coefficient C_u where

$$C_u\equiv\frac{u_*}{u_m}, \qquad (26)$$

and the heat-transfer coefficient C_θ where

$$C_\theta\equiv\frac{(-\overline{w'\theta'_v})_a}{[u_*(\theta_{vm}-\bar{\theta}_{vs})]}, \qquad (27)$$

455-016 O - 72 - 3

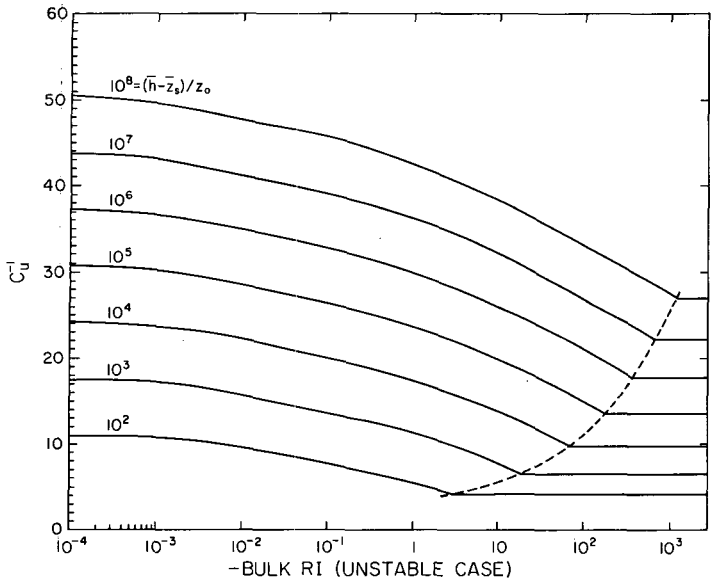

FIGURE 2.—The inverse of the friction coefficient, $C_u=u_*/u_m$, as a function of the negative bulk Richardson number in the unstable case. The free convection regime is estimated to commence to the right of the dashed curve.

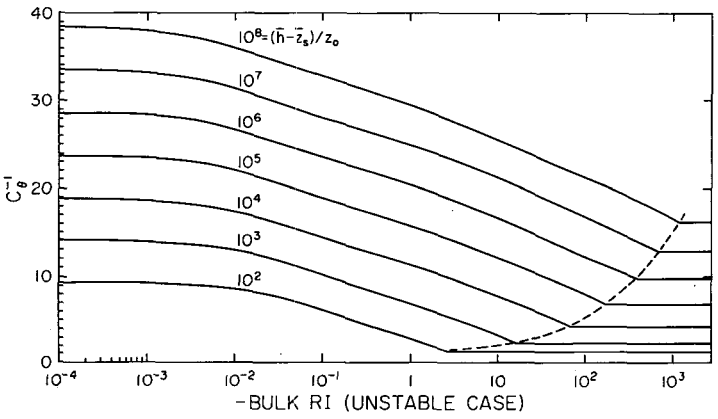

FIGURE 3.—The inverse of the heat-transfer coefficient, $C_\theta=\overline{w'\theta_v'}/[u_*(\bar{\theta}_{vs}-\theta_{vm})]$, as a function of the negative bulk Richardson number in the unstable case.

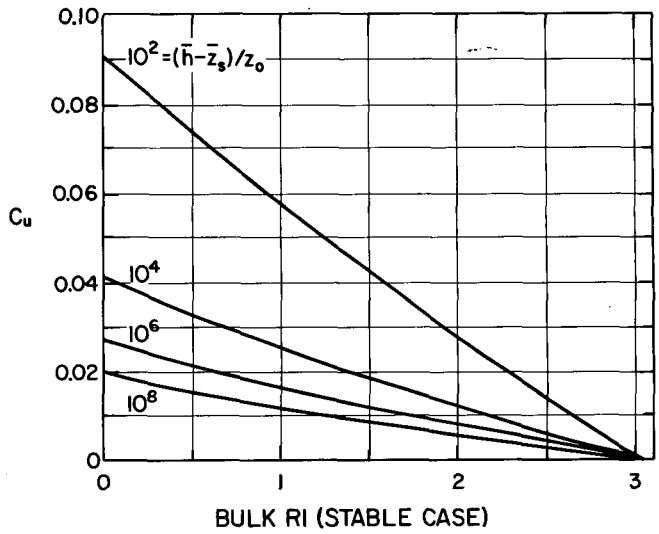

FIGURE 4.—The friction coefficient, C_u, as a function of the bulk Richardson number in the stable case.

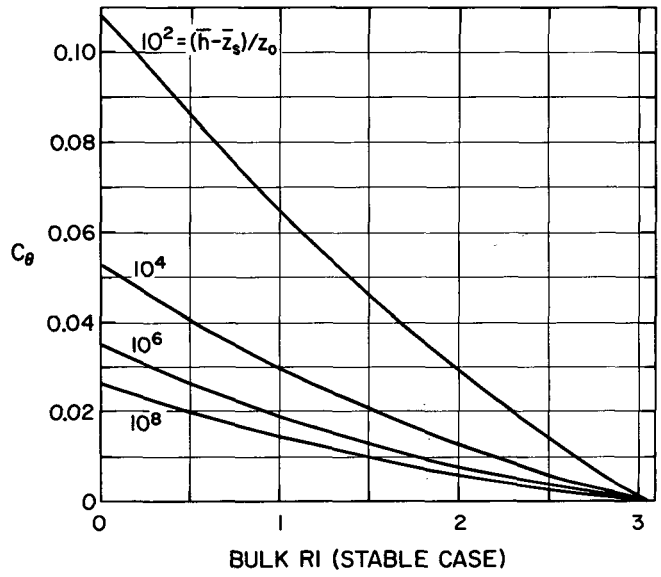

FIGURE 5.—The heat-transfer coefficient, C_θ, as a function of the bulk Richardson number in the stable case.

as unique functions of the available quantities $(\bar{h}-\bar{z}_s)/z_0$ and $\mathrm{Ri_B}$. This was effected by specifying $(\bar{h}-\bar{z}_s)/z_0$ and $(\bar{h}-\bar{z}_s)/L$ and then solving eq (25) numerically for $\mathrm{Ri_B}$, solving eq (20) and (23) for C_u, and solving eq (21), (22), and (24) for C_θ.

For the unstable case, C_u^{-1} and C_θ^{-1} are shown in figures 2 and 3, and for the stable case, C_u and C_θ are shown in figures 4 and 5. In the former case, inverse values of the desired coefficients are shown because the influence of the logarithm of $(\bar{h}-\bar{z}_s)/z_0$ is then seen to be approximately additive.

For curve-fitting purposes, the unstable case may be approximated by

$$C_u=[C_{uN}^{-1}-25\exp(0.26\zeta-0.030\zeta^2)]^{-1} \tag{28}$$

and

$$C_\theta=(C_{\theta N}^{-1}+C_u^{-1}-C_{uN}^{-1})^{-1} \tag{29}$$

where

$$\zeta=\log_{10}(-\mathrm{Ri_B})-3.5 \text{ and } \mathrm{Ri_B}<0, \tag{30}$$

and the stable case by

$$\left.\begin{aligned} C_u&=C_{uN}\left(1-\frac{\mathrm{Ri_B}}{\mathrm{Ri_C}}\right) \qquad (31)\\ \text{and}\qquad C_\theta&=C_{\theta N}\left(1-\frac{\mathrm{Ri_B}}{\mathrm{Ri_C}}\right) \qquad (32)\end{aligned}\right\} 0\le\mathrm{Ri_B}\le 0.9\mathrm{Ri_C}$$

where C_{uN} and $C_{\theta N}$ are the neutral values of the coefficients given by

$$C_{uN}=\{k^{-1}\log_e\left[\frac{0.025(\bar{h}-\bar{z}_s)}{z_0}\right]+8.4\}^{-1} \tag{33}$$

and

$$C_{\theta N}=\{k^{-1}R\log_e\left[\frac{0.025(\bar{h}-\bar{z}_s)}{z_0}\right]+7.3\}^{-1} \quad (34)$$

and $\mathrm{Ri_C}$ is a critical bulk Richardson number given by

$$\mathrm{Ri_C}=3.05. \quad (35)$$

The existence of $\mathrm{Ri_C}$ in eq (31) and (32) is not surprising since the log-linear formulation is known to produce a critical value of the local Richardson number in the surface layer. However, it is not realistic to expect $\mathrm{Ri_B}$ ever to exceed critical. With any mean flow at all near a rough surface, a turbulent region is expected to exist even though it might be extremely shallow. If $\mathrm{Ri_B}$ obtained from eq (25) ever exceeds $\mathrm{Ri_C}$, one would probably have to conclude that $\bar{h}-\bar{z}_s$ had been calculated to be too large. To avoid this situation, it is suggested that $\mathrm{Ri_B}$ not be allowed to exceed an arbitrary value of about 0.9 $\mathrm{Ri_C}$, as in eq (31) and (32). In this manner, unrealistic zero values of C_u and C_θ will be avoided, and surface fluxes will generally be finite. Zero values for the surface fluxes would render the length L indeterminate, and we will assume later that the value for L forms the basis for the estimate of $\bar{h}-\bar{z}_s$ in stable conditions.

The vertical flux of virtual potential temperature obtained from eq (27) and (29) or (32) may be partitioned into the kinematic sensible heat and moisture fluxes as follows, using eq (3):

$$(\overline{w'\theta'})_a=\frac{(\bar{\theta}_s-\theta_m)(\overline{w'\theta'_v})_a}{\bar{\theta}_{vs}-\theta_{vm}} \quad (36)$$

and

$$(\overline{w'q'})_a=\frac{(\bar{q}_s-q_m)(\overline{w'\theta'_v})_a}{\bar{\theta}_{vs}-\theta_{vm}}. \quad (37)$$

Figures 2–5 indicate that for commonly occurring values of $\mathrm{Ri_B}$, the principal variable that can cause C_u and C_θ to change substantially is z_0, that may range over four or five orders of magnitude. Probably the greatest absolute uncertainly of these values for C_u and C_θ, therefore, is uncertainly in z_0 associated with roughness elements taller than the height of the surface layer, such as hills, cities, and mountains of horizontal scale less than a horizontal grid length of the GCM. It is assumed here that the surface-layer formulations utilized will still be approximately valid if "effective" roughness lengths are used in these cases, as have been estimated by Fiedler et al. (1971).

For some purposes, it may be of interest to obtain $(\bar{h}-\bar{z}_s)/L$, given observations from which $\mathrm{Ri_B}$ has been deduced. From the definitions of L, $\mathrm{Ri_B}$, C_u, and C_θ, it may be shown that

$$\frac{(\bar{h}-\bar{z}_s)}{L}=\left(\frac{kC_\theta}{C_u^2}\right)\mathrm{Ri_B}. \quad (38)$$

In figures 2–5 we find that $(\bar{h}-\bar{z}_s)/L$ typically ranges from eight to 30 times larger than $\mathrm{Ri_B}$ with the ratio being greater for stable conditions and for larger values of $(\bar{h}-\bar{z}_s)/z_0$.

Free Convection

The limiting case of free convection must be considered with respect to a GCM parameterization even though the case may never seem to occur during measurements at a fixed point within the surface layer. The dashed curves on the right of figures 2 and 3 are estimates of the region where essentially free convection commences, based upon the following treatment. In the numerical model of Deardorff (1970*b*), it was noticed that for strong instability the root-mean-square wind speed at z_a, denoted by $\sigma(u_a)$, is given approximately by

$$\sigma(u_a)=0.7w_* \quad (39a)$$

where

$$w_*=\left[\left(\frac{g}{\theta_{vm}}\right)(\overline{w'\theta'_v})_a(\bar{h}-\bar{z}_s)\right]^{1/3} \quad (39b)$$

is the convective velocity scale discussed by Deardorff (1970*c*). The velocity fluctuations contributing most to $\sigma(u_a)$ for large values of $-(\bar{h}-\bar{z}_s)/L$ were of sufficiently large scale to persist with a given sign at a fixed point for periods of 20 min or more in typical circumstances, and were associated much more with the free convection than with the low level wind shear. Thus, even for truly free convection with $\bar{u}_a=0$, an apparent friction velocity would be measured at a fixed point and would be associated with a time-mean velocity of magnitude $\sigma(u_a)$ on the average. Upon replacement of $\bar{u}_a$ in eq (10) with $\sigma(u_a)$, numerically solving eq (10), (11), and (12), and again relating $(\bar{h}-\bar{z}_s)/L$ to $\mathrm{Ri_B}$, the free-convection region of figures 2 and 3 was established. The region commences considerably before eq (20) and (21) would break down if ever $-L/z_0$ is not much greater than unity.

For $\mathrm{Ri_B}$ in the vicinity of, or exceeding, the value indicative of the commencement of free convection, C_u and C_θ based on the area-averaged wind are not known with any accuracy. However, the mean wind must be so small in this case that some inaccuracy in C_u may be tolerated. Here, C_u and C_θ are maintained constant, as in figures 2 and 3, for $-\mathrm{Ri_B}$ lying within the free-convection regime. The regime defined in the above manner is most simply identified, numerically, by testing if C_u^{-1} and C_θ^{-1} are less than about 0.5 and 0.3 of their respective neutral values.

For the heat flux, this procedure is not entirely adequate. Instead, the virtual-temperature heat flux, obtained by multiplying C_θ by u_* $(\bar{\theta}_{vs}-\theta_{vm})$ in the unstable case, should be constrained further to be no smaller than Townsend's (1964) free-convection heat flux given, for virtual potential temperature, by

$$\overline{w'\theta_v'}_{\substack{\mathrm{FREE}\\ \mathrm{CONV}}}=0.20\left(\frac{\kappa^2 g}{\nu\theta_{vm}}\right)^{1/3}(\bar{\theta}_{vs}-\theta_{vm})^{4/3} \quad (40a)$$

$$=0.19(\bar{\theta}_{vs}-\theta_{vm})^{4/3}\mathrm{cm\cdot deg\cdot s^{-1}} \quad (40b)$$

where κ is the molecular thermal diffusivity for heat or moisture, and ν is the kinematic viscosity. The relationship given in eq (40a) was confirmed by Deardorff et al. (1969) for experiments on penetrative convection in water

using the appropriate coefficient of volumetric expansion. This coefficient has also been used by Leovy and Mintz (1969) for the case of strong instability in a simulation of the Martian atmosphere.

4. THE ANGLE OF THE SURFACE WIND

This angle must be determined so that u_m in eq (25) and (26) may be obtained knowing $|\mathbf{V}_m|=(U_m^2+V_m^2)^{1/2}$. The reason why u_m appears in $\mathrm{Ri_B}$, rather than $|\mathbf{V}_m|$, is that the surface stress relates to the component of the wind along the direction at the surface as in eq (10) or (13). The two wind speeds are related by

$$u_m=|\mathbf{V}_m|\cos(\psi_m-\psi_x) \tag{41}$$

where ψ_m is the angle between the X-axis and $\mathbf{V}_m$, and ψ_x is the unknown angle of the x-axis toward which u_a points. Of course, ψ_x must also be determined so that the surface stress components τ_{sX} and τ_{sY} be known; that is,

$$\tau_{sX}=\rho_s u_*^2\cos\psi_x \text{ and } \tau_{sY}=\rho_s u_*^2\sin\psi_x \tag{42}$$

where it is assumed that the direction of the surface stress is the same as that of the surface wind.

Present GCMs ignore the turning of the wind between $\bar{u}_a$ and that at the lowest interior grid level or combination of lowest two levels. In the model of Smagorinsky et al. (1965), there is usually sufficient vertical resolution to justify this procedure. The method to be described here is for use with GCMs of poorer vertical resolution and is based upon the assumption that $\bar{h}-\bar{z}_s$ is known.

The procedure will be to determine $-(\partial\bar{p}/\partial x)_s$, the horizontal pressure gradient along the x-direction at the surface. Then, knowing $(\nabla_H\bar{p})_s$ from the GCM output, the direction of the x-axis may be deduced.

The Pressure Gradient Along x at the Surface

If the x-component of the equation of motion is applied at $z=\bar{z}_a$, we obtain the familiar relation

$$\left(\frac{\partial\bar{p}}{\partial x}\right)_s\approx\left(\frac{\partial\bar{p}}{\partial x}\right)_a=\left(\frac{\partial\tau_x}{\partial z}\right)_a. \tag{43}$$

Since $\bar{v}=0$ at $z=\bar{z}_a$, eq (43) neglects only the acceleration terms which are relatively small at this level where the stress gradient is large. Although τ_x is sometimes thought to be constant with height in the shallow surface layer, it usually decreases with height through this layer as rapidly or more rapidly than at higher levels. This point is illustrated by the profile of $\overline{u'w'}/u_*^2$ obtained from the numerical model (Deardorff 1970*a*) for the neutral PBL, shown in figure 6. With $-(\bar{h}-\bar{z}_s)/L$ comparable to or greater than 1.5, τ_x was found to be distributed nearly linearly with height between the surface and a simulated inversion base at $z=\bar{h}=z_i$. The distribution obtained when $-(\bar{h}-\bar{z}_s)/L=45$ is also shown in figure 6. (A small positive value for $\overline{u'w'}$ probably occurs at levels near z_i but was suppressed numerically by the restriction that $w=0$ at $z=z_i$.)

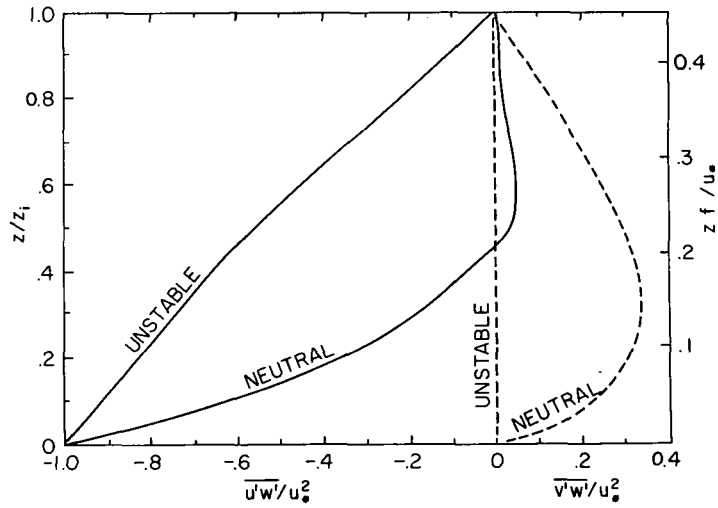

FIGURE 6.—Numerically derived vertical profiles of Reynolds stress components: solid curves are $\overline{u'w'}/u_*^2$, and dashed curves are $\overline{v'w'}/u_*^2$. The unstable case is for $-z_i/L=45$, where z_i is the height of a simulated inversion base and L is the Monin-Obukhov length.

These results suggest that $(\partial\bar{p}/\partial x)_s$ is given by

$$-\left(\frac{1}{\rho}\frac{\partial\bar{p}}{\partial x}\right)_s=\frac{cu_*^2}{\bar{h}-\bar{z}_s} \tag{44}$$

where c is a decreasing function of thermal instability given by

$$c=1.0+1.8\exp\left[\frac{0.2(\bar{h}-\bar{z}_s)}{L}\right] \tag{45a}$$

in the unstable and neutral cases. In the latter case, a value of 2.8 is obtained for c based upon the definition that $(\bar{h}-\bar{z}_s)_N=0.35\ u_*/f$.

For stable cases, little is known about the vertical profiles of the stress components except that these components approach zero at a height that is a smaller fraction of u_*/f than for the neutral case. A shape-preserving assumption will here be made for τ_x; that is, that the effect of stable stratification upon eq (44) is contained wholly in its effect upon $\bar{h}$. Hence,

$$c=2.8 \text{ (stable case)} \tag{45b}$$

also. The measurements of Clarke (1970*a*) are not inconsistent with this viewpoint, and those of Lettau and Dabberdt (1970), during very stable conditions when $\bar{h}-\bar{z}_s=32$ m, support it remarkably well.

In eq (44), it is assumed that the magnitude of $\overline{u'w'}$ existing at $z=\bar{h}$ and associated with free-tropospheric processes such as gravity-wave momentum transfer or clear-air turbulence is negligible in comparison with u_*^2. This assumption need not be made, however, and an estimate for the free-tropospheric value of $(\overline{u'w'})_h$ may be added to u_*^2 in eq (44).

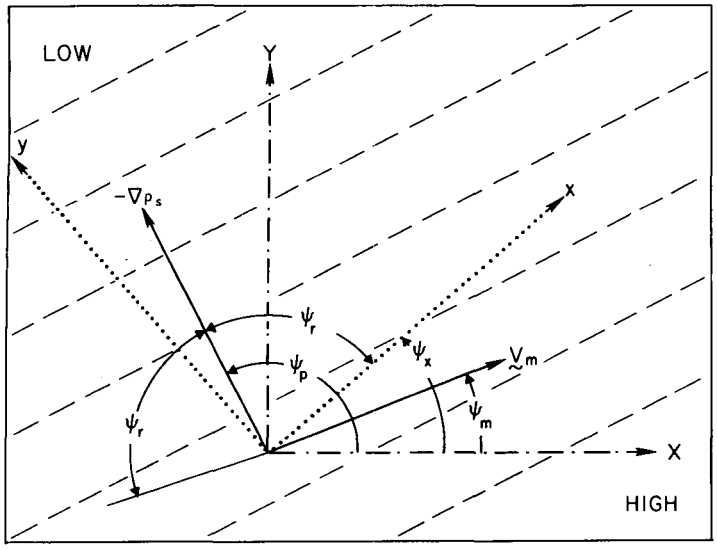

FIGURE 7.—Relationships between angles ψ_p, ψ_m, ψ_r, and ψ_x. Dashed lines are isobars.

Direction of x-Axis

With the condition

$$\left(\frac{\partial \bar{p}}{\partial x}\right)_s^2 \leq (\nabla_H \bar{p})_s^2 \tag{46}$$

always satisfied (it may occasionally have to be enforced numerically), the relative angle ψ_r between the direction of $(-\nabla_H \bar{p})_s$ and the x-axis is obtainable from

$$\psi_r \equiv |\psi_p - \psi_x| = \cos^{-1}\left[\frac{-(\partial \bar{p}/\partial x)_s}{|\nabla_H \bar{p}|_s}\right] \tag{47}$$

where $0 \leq \psi_r \leq \frac{1}{2}\pi$. See figure 7 for schematic definitions of ψ_p and the relations between the various angles and the x,y- and X,Y-axes. Except for ψ_r the angles range up to $\pm\ \pi$ from the eastward pointing X-axis. The angle ψ_p is obtainable from

$$\psi_p = \tan^{-1}\left[\frac{-(\partial \bar{p}/\partial Y)_s}{(\partial \bar{p}/\partial X)_s}\right]. \tag{48}$$

Since

$$\psi_x = \psi_p \pm \psi_r, \tag{49}$$

some criterion must be selected for choosing the proper sign. Although the sign could be chosen that points the x-axis most nearly along the geostrophic flow direction, this procedure would be indeterminate at the Equator and probably unrealistic within $\pm$ 5° or 10° of the Equator. Instead, the sign that minimizes the angle between ψ_x and the mean PBL flow direction, ψ_m, will be chosen here. The latter angle is given by

$$\psi_m = \tan^{-1}\left(\frac{V_m}{U_m}\right). \tag{50}$$

Thus, if ψ_x^+ and ψ_x^- are the two possibilities for ψ_x from eq (49), we select ψ_x^+ if $|\psi_x^+ - \psi_m| < |\psi_x^- - \psi_m|$. Otherwise, we select ψ_x^-.

Subsequently, u_m^2 is obtained from eq (41), and if it differs by more than 15 percent, for example, from the value previously assigned or assumed, then the bulk Richardson number is to be recalculated, and revised values of the fluxes and of ψ_x should be obtained as an iteration. It has been found that the iteration is rarely necessary in the unstable case, but that one is sometimes needed in the stable case. An iteration in the latter case can sometimes be avoided by starting with the assumption that $u_m^2 = 0.9(U_m^2 + V_m^2)$ in anticipation of a significant difference in flow angles between u_a and $\mathbf{V}_m$.

A difficulty was originally encountered whenever $\bar{h} - \bar{z}_s$ was quite small and u_* was estimated to be relatively large. Then eq (44)–(50) would cause ψ_x to be nearly equal to ψ_p, and u_m would be drastically reduced after application of eq (41). In the iteration, u_* would therefore be estimated to be much smaller and thus ψ_x would be predicted to be nearly equal to ψ_m, etc. Such iterative oscillations were avoided by utilizing for u_* in eq (44) the average of the existing and previous estimate and by restricting u_m to be no less than some fraction of $|\mathbf{V}_m|$ such as 0.71. This restriction corresponds to a maximum cross-flow angle between u_a and $\mathbf{V}_m$ of 45° although it is u_m which is restricted here rather than $\psi_x - \psi_m$.

The method of this section incorporates most of the effect of baroclinic turning of the wind between levels $\frac{1}{2}(\bar{h} + \bar{z}_s)$ and $\bar{z}_s$, since the surface flow-angle calculation is based upon the surface pressure pattern, among the other factors. It also avoids the inconsistency of other methods which do not make use of the surface pressure pattern. In those methods, a wind at "anemometer" level estimated by downward extrapolation from higher levels could frequently be blowing toward higher surface pressure rather than lower.

5. PROGNOSTIC EQUATION FOR $\bar{h}$

The Unstable Case

The reason why $\bar{h}(X,Y,t)$ must be treated as time dependent in the unstable case is that the existing height of an inversion base at $\bar{h} = z_i$, that confines the PBL, depends upon its past height. Only its rate of change with time can be calculated. The proposed prognostic equation is

$$\frac{\partial \bar{h}}{\partial t} = \overline{W}_h - \overline{\mathbf{V}}_h \cdot \nabla \bar{h} + S + \nabla \cdot (K \nabla \bar{h}) \tag{51}$$

where $\overline{W}_h$ is the vertical velocity at level $\bar{h}$ obtained from the GCM, $\overline{\mathbf{V}}_h \cdot \nabla \bar{h}$ is the advective term, S is the source term associated with penetrative convection, and the last term, involving an eddy coefficient K, represents (at least partly) effects of subgrid-scale lateral diffusion of $\bar{h}$. Except for the last term, this equation expresses the idea that an average fluid particle initially located at

$z=z_i$ remains at z_i unless entrainment causes z_i to increase by means of the term S.

If $\bar{h}$ lies below the level z_2 (see fig. 1), then $\overline{W}_h$ in eq (51) needs to be interpolated between the GCM value at z_2 and the terrain-induced value at z_s. For $z_2 < \bar{h} < z_4$, the GCM vertical velocities at z_2 and z_4 must be interpolated for $\overline{W}_h$, etc.

A refinement is possible if the GCM incorporates a cumulus parameterization from which the average cumulus updraft speed W_C and cloud-cover ratio r_C at $z=\bar{h}$ may be estimated. From this information, the average vertical velocity $\overline{W}_{ho}$ in the air *outside* of such clouds may be obtained [$\overline{W}_{ho}=\overline{W}_h-r_C W_C/(1-r_C)$]. The definition of the PBL has not here included the region of turbulence within towering cumuli but only the average height of surface-induced turbulent fluxes outside of such clouds. Therefore, $\overline{W}_{ho}$ is more appropriate than $\overline{W}_h$ in eq (51) and tends to be slightly more negative.

In the horizontal advection term, the suggestion is made that $\bar{V}_h$ can be replaced by $\bar{V}_m$ because of the thorough vertical mixing in the unstable case.

The source term, S, represents the rate of entrainment of stable air above z_i into the convectively mixed layer below. Two different expressions are available for this rate. Lilly (1968) has shown that when the inversion base at z_i is sufficiently pronounced that an inversion strength $\Delta\theta_{vi}$ can be defined, the following expression holds in the absence of liquid water:

$$S=\frac{-(\overline{w'\theta_v'})_i}{\Delta\theta_{vi}}\approx\frac{0.1(\overline{w'\theta_v'})_a}{\Delta\theta_{vi}} \tag{52}$$

where $(\overline{w'\theta_v'})_i$ is the flux of virtual potential temperature at $z=z_i=\bar{h}$, and $\Delta\theta_{vi}$ is the virtual potential temperature "jump" in passing from the mixed layer with $\bar{\theta}_v=\theta_{vm}$ to the nearly laminar air just above having $\bar{\theta}_v=\theta_v^+$. For the case when $\theta_v=\theta$, some approximate measurements are available (see Deardorff et al. 1969) that suggest the factor 0.1 in the right-hand expression of eq (52). The estimate for $\Delta\theta_{vi}$ is even less certain. Here we suggest that $\Delta\theta_{vi}\equiv\theta_v^+-\theta_{vm}$ be obtained with aid of a downward extrapolation from the closest grid value lying above $z=\bar{h}$ as follows:

$$\Delta\theta_{vi}=\theta_{v1}-\gamma_\theta(z_1-\bar{h})-\theta_{vm} \tag{53a}$$

when $\bar{h}\le z_1$, and

$$\Delta\theta_{vi}=\theta_{v3}-\gamma_\theta(z_3-\bar{h})-\theta_{vm} \tag{53b}$$

when $z_1\le\bar{h}\le z_3$, etc. The parameter γ_θ is a standard virtual potential temperature increase rate, which may be assigned a value of about 4×10^{-5} °C/cm. If θ_{vm} could be determined independently of θ_{v1} and θ_{v3}, as suggested in section 2, this method for estimating $\Delta\theta_{vi}$ would be more satisfactory.

The second method for estimating the rate of penetrative convection is the method used by Deardorff et al. (1969) in a set of experiments for which $\Delta\theta_i$ was sometimes too small to estimate. If the temperature used in their case for convection in water is replaced by θ_v, and if the factor of 0.1 in eq (52) is used, their formulation becomes slightly revised to

$$S=\frac{1.1(\overline{w'\theta_v'})_a}{[(\bar{h}-\bar{z}_s)\partial\theta_v^+/\partial z]} \tag{54}$$

where the superscript $^+$ indicates evaluation at a height just above any jump in $\overline{\theta_v}$. As an estimate of $\partial\theta_v^+/\partial z$, it is here suggested that γ_θ be used. Equation (54) can be rewritten as

$$S=\frac{0.1(\overline{w'\theta_v'})_a}{\Delta\theta_{vi}'} \tag{55}$$

where

$$\Delta\theta_{vi}'=0.09(\bar{h}-\bar{z}_s)\gamma_\theta \tag{56}$$

It is reasonable to expect that eq (55) will be more accurate than eq (52) when $\Delta\theta_{vi}$ is small, and vice versa. Hence, it is suggested that eq (52) be used if $\Delta\theta_{vi} > \Delta\theta_{vi}'$; otherwise that eq (54) be used.

The circumstance in which a shallow stratocumulus cloud deck occupies the upper portion of the PBL has been treated by Lilly (1968), but adds too many complications to be considered here.

The eddy-coefficient term in eq (51) formally represents the subgrid-scale lateral mixing associated with $-\overline{V_h'\cdot\nabla h'}$. It may in addition represent smoothing necessary to offset adverse numerical effects arising from a spatial distribution of S that may have small-scale irregularities. The eddy coefficient K will here be estimated by the nonlinear formulation of Smagorinsky (1963):

$$K=c_1^2\Delta X\Delta Y\left[2\left(\frac{\partial U_m}{\partial X}\right)^2+2\left(\frac{\partial V_m}{\partial Y}\right)^2+\left(\frac{\partial V_m}{\partial X}+\frac{\partial U_m}{\partial Y}\right)^2\right]^{1/2} \tag{57}$$

where c_1 is uncertain but is tentatively set at 0.2 (see Miyakoda et al. 1970). An abbreviated form of eq (57) involving absolute magnitudes may be equally satisfactory in view of other uncertainties, including whether or not a K term is even appropriate.

The time-dependent approach involving eq (51) has previously been used by Lavoie et al. (1970), although they set S to zero whenever $\Delta\theta_i$ was finite, and also set K to zero.

The Stable Case

In this case, there is probably too little known about $\bar{h}$ to allow use of an equation for $\partial\bar{h}/\partial t$. The PBL depth is then often small in comparison with $0.35u_*/f$ and not likely to be much affected by vertical velocity and advection at the top of the PBL where, by definition, little turbulence exists. Furthermore, a time-dependent equation would have difficulty in causing $\bar{h}$ to collapse from a large to a small value upon development of a cool underlying surface. Instead, the following interpolation formula

between the neutral-stability value, $0.35u_*/f$, and a value proportional to L is proposed:

$$\bar{h}-\bar{z}_s=\left(\frac{1}{30L}+\frac{f}{0.35u_*}+\frac{1}{z_{\mathrm{TROP}}}\right)^{-1} \tag{58}$$

where z_{TROP} is the height of the tropopause. This latter term is added only to ensure that if exactly neutral conditions were ever to occur near the Equator, $\bar{h}$ would not exceed z_{TROP}. The addition of inverse values in eq (58) ensures that the singular case $f=0$ otherwise causes no difficulty, and the use of $\mathrm{Ri_B}\leq 0.9\ \mathrm{Ri_C}$ in eq (31) and (32) ordinarily ensures that L and u_* remain finite.

In very stable conditions, the first term within the parentheses in eq (58) dominates the others. Then $\bar{h}-\bar{z}_s\approx 30L$, with the proportionality constant having been very roughly estimated from the study of Clarke (1970*a*) and Lettau and Dabberdt (1970). From the latter study, it appears very reasonable to conclude that the depth of the stable PBL becomes essentially independent of u_*/f when $L\ll 0.35u_*/f$. This stable limit, with the aid of eq (38) and figures 4 and 5, implies that $\mathrm{Ri_B}$ then has a value of order unity.

For compatibility with eq (51), $\bar{h}$ from eq (58) is also considered to apply at time $t+\Delta t$. Thus, initial values for $\bar{h}-\bar{z}_s$, such as 1 km, are needed at all grid points of the GCM.

The possibility that a well mixed but slightly stable PBL has its depth limited by strong thermal stratification just above $z=\bar{h}$ is here discounted because of the observations of Clarke (1970*a*) that showed the inversion in the stable case to be based only at the surface.

A more rigorous approach for the height of the stable boundary layer would be to set $\bar{h}-z_s$ to a small value such as 50 m whenever $\theta_{vs}-\theta_{vm}$ switches from positive to negative, and then to allow $\bar{h}$ to grow upward at a rate proportional to u_*. Available evidence suggests this rate is typically $S=0.05u_*$. However, the constant of proportionality, 0.05, is presently very uncertain and is probably a function of $(\bar{h}-\bar{z}_s)/L$.

Limits of $\bar{h}$

If $\bar{h}-\bar{z}_s$ fails to remain much larger than z_0, several relationships used in this study would break down. Therefore, it is suggested that the minimum value

$$h_{min}=\bar{z}_s+50z_0 \tag{59}$$

be enforced under all conditions.

In the presence of trade-wind cumuli or fair weather cumuli in general, the lifting condensation level probably acts as an upper limit to $\bar{h}$. The limiting mechanism is the export (detrainment) of boundary layer air into clouds that are growing, along with the compensating subsidence between clouds. This mechanism should be incorporated into the equation for $\bar{h}$ when enough is known to parameterize the vertical transports of moisture, heat, and momentum by the clouds whose bases are near $z=\bar{h}$.

6. THE PBL FLUXES WHEN $\bar{h}$ IS LARGE

If $\bar{h}$ lies above z_2 (see fig. 1), a significant vertical flux may exist at this level and need to be taken into account in the GCM equations. Values of $\overline{U'W'}$, $\overline{V'W'}$, $\overline{W'\theta'}$, and $\overline{W'q'}$ centered at the level z_2 or z_4 can then be thought of as the sum of a contributuion from the equilibrium PBL flux and the free atmospheric vertical flux. For the PBL portion, the stress profile of τ_x shown in figure 6, along with what information exists about heat flux profiles from studies of Telford and Warner (1964), Lenschow and Johnson (1968), Clarke (1970*a*), and Lenschow (1970), suggests that in the unstable case

$$\overline{U'W'}(\hat{z})=-u_*^2(1-\hat{z})\cos\psi_x, \tag{60}$$

$$\overline{V'W'}(\hat{z})=-u_*^2(1-\hat{z})\sin\psi_x, \tag{61}$$

$$\overline{W'\theta'}(\hat{z})=(\overline{W'\theta'})_a(1-\hat{z}), \tag{62}$$

and

$$\overline{W'q'}(\hat{z})=(\overline{w'q'})_a(1-\hat{z}) \tag{63}$$

where

$$\hat{z}=\frac{z-\bar{z}_s}{\bar{h}-\bar{z}_s}. \tag{64}$$

In these equations, $z=z_2$ if $h>z_2$; $z=z_4$ also if $\bar{h}>z_4$. A simplification that has been made in eq (60) and (61) is that $\overline{v'w'}$ $(\hat{z})$, which must exist for some small interval above the inversion base at $\hat{z}=1$, can be ignored and only $\overline{u'w'}$ taken into account. (The absence of $\overline{v'w'}$ below $z=\bar{h}$ for a significant degree of instability is associated with the absence of appreciable shear, $\partial\bar{v}/\partial z$, in the mixed region.) A second simplification is the assumed linearity and monotonic distributions for all the PBL fluxes.

In the neutral or stable case, the momentum flux $\overline{v'w'}$ cannot be ignored. From figure 6, $\overline{u'w'}$ and $\overline{v'w'}$ may be approximated by

$$\overline{u'w'}=-u_*^2(1-2.80\hat{z}+2.39\hat{z}^2-0.61\hat{z}^3) \tag{65}$$

and

$$\overline{v'w'}=-u_*^2(1.83\hat{z}-2.91\hat{z}^2+1.20\hat{z}^3)\frac{v_m}{v_{mN}} \tag{66}$$

where

$$v_m=-U_m\sin\psi_x+V_m\cos\psi_x \tag{67}$$

and

$$v_{mN}=5u_*. \tag{68}$$

Polynomials are used here, rather than exponentials and sinusoids, for greater computer efficiency. In eq (60)–(66), $\hat{z}$ is restricted to be less than unity.

In eq (66), the ratio v_m/v_{mN} is appended to guarantee the correct sign irrespective of hemisphere and to allow for the fact that v_m will frequently deviate from the value for neutral, barotropic, and equilibrium conditions. Under such ideal conditions, v_m was found (Deardorff 1970*a*) to have the magnitude of v_{mN} given in eq (68).

TABLE 3.—*Computer time required for various parts of a simulated GCM having a parameterized boundary layer*

Calculation of	Computer (CPU) time per grid point	Fraction of total
	(ms)	%
PBL mean values, eq (1)	0. 02	5
Eddy coefficient, eq (57)	. 02	5
Stress components and vertical fluxes	. 13	32
Angle of surface wind	. 15	36
Predicted value of $\bar{h}$	. 09	22
Total	0. 41	100

Thus, if baroclinicity causes a stronger than average veering of the wind in the PBL, this would be manifested in a larger (negative) value of v_m (in the Northern Hemisphere), a larger value of $-\partial\bar{v}/\partial z$ in the PBL, and a larger positive value of $\overline{v'w'}$ within the PBL using eq (66)–(68). The effect of stable stratification is included implicitly in eq (65) and (66) in its effect upon $\bar{h}-\bar{z}_s$. These equations are converted to the X, Y system by

$$\overline{U'W'}=\overline{u'w'}\cos\psi_x-\overline{v'w'}\sin\psi_x \tag{69}$$

and

$$\overline{V'W'}=\overline{u'w'}\sin\psi_x+\overline{v'w'}\cos\psi_x. \tag{70}$$

The heat flux profile by Clarke (1970*a*) for stable stratification suggests a linear distribution in this case also, so that eq (62) and (63) will be assumed to hold in stable conditions as well. However, the height of the PBL is not expected to exceed z_2 nearly as often in stable conditions as in unstable conditions.

The estimates of the vertical fluxes caused by intermittent mixing processes within the free atmosphere are to be added to the right-hand sides of eq (60)–(63) or eq (69) and (70).

7. RESULTS OF NUMERICAL TESTING OF THE PARAMETERIZATION

The preceding method for estimating the surface fluxes and PBL height was tested preliminarily for completeness and efficiency [although a more complicated, time-dependent formulation was used in place of eq (58) in stable cases]. The numerical program utilized simulated GCM data held constant in time.

An approximation for the sake of efficiency was the replacement of $\cos(\psi_m-\psi_x)$ in eq (41) by $[1-0.5\times(\psi_m-\psi_x)^2]$. The approximation is good because the angular difference was usually of order 10° to 15° and was constrained to be less than 45°.

The timing of various portions of the program per average gridpoint of the horizontal array (30×40) is given in table 3. Calculations were performed on the International Business Machines 360/91 computer at the University of California, Los Angeles (UCLA). In the tests, the heat flux was directed upward over about two-thirds of the region, which extended over both hemispheres, and downward in the remainder. The total time of 0.41 ms per gridpoint may be compared with the value 3.6 ms per horizontal gridpoint for each time step of the three-level GCM of Arakawa et al. (1969) run on the same computer or to 1.2 ms per gridpoint within the full three-dimensional array of gridpoints. Thus, inclusion of the methods presented here in such a GCM would be about equivalent to the addition of one-third of another horizontal level of gridpoints. It is estimated that this value would at most be doubled if PBL mean values for θ_m and q_m were obtained from separate time-dependent equations and if allowance were made for occasional presence of a stratocumulus cloud cover capping the PBL in the calculations for S in eq (51).

No attempt was made to determine the relative computer time spent in obtaining the interior PBL fluxes when $\bar{h}$ was large (sec. 6). However, it may be noted that the fraction would be quite small because the sine and cosine calculations that occur will have been performed previously and stored.

In the numerical tests, $\bar{h}-\bar{z}_s$ reached essentially equilibrium values within the first 2 hr of simulated time except in regions of upward heat flux *and* upward vertical motion at $z=\bar{h}$. In the latter regions, $\bar{h}$ was still increasing at the end of 15 hr, from an initial value of z_s+800 m, at a rate only slightly greater than $\overline{W}_h$. No provision was made in the test to restrict $\bar{h}$ to the lifting condensation level determined from values of θ_m and q_m because of the artificiality of the statically simulated GCM data.

8. DISCUSSION OF UNCERTAINTIES

It is all too apparent when attempting a parameterization of this kind that far too little information is available on the PBL. Many assumptions had to be made. However, we feel that the general procedure described for obtaining the surface fluxes and the height of the PBL is valid in most circumstances, and it should be possible to improve each assumption without altering the basic approach as more information becomes available.

One area of uncertainty which could stand much research concerns the best definition for the top of the surface layer, $\bar{z}_a$. Although it makes sense that $\bar{z}_a-\bar{z}_s$ should be some small fraction of $\bar{h}-\bar{z}_s$ rather than some fixed height, it is not clear whether some fraction other than 0.025 might not be more appropriate. The fraction should be sufficiently small that below $\bar{z}_a$ the air-to-surface differences normalized as in this paper are functions of z/z_0 and z/L, and not of $z/\bar{h}$ and $\bar{h}/L$. It should also be small enough that the vertical flux in question is not much different than at the surface. Yet, the fraction should *not* be so small that the dimensionless differences between heights $\bar{h}$ and $\bar{z}_a$ depend upon $\bar{h}/z_0$. It is probable that both requirements cannot be jointly satisfied well at $z=\bar{z}_a$ above terrain having roughness elements extending up to a significant fraction of $\bar{h}$. It may be necessary to utilize a displacement height as well as a roughness length.

Another area of equal uncertainty concerns the distinction between the upper part of the PBL and the base of the free atmosphere, especially with regard to the role played by baroclinicity. Sheppard (1958) has emphasized the possibility that the frictional layer may extend throughout the troposphere when a strong, monotonically directed thermal wind shear exists up to the usual level of the jet stream. In such circumstances, very little turning of the wind would be expected at low levels. This possibility is included in the present analysis through eq (44) and (51) when the PBL is unstably stratified so that $\bar{h}$ may become large (if no strong inversion or subsidence restricts it). If the PBL is stably stratified, no allowance is made in eq (58) for thermal wind shear to cause the PBL height to be larger than otherwise. Even in that case, however, the addition of a thermal-wind shear stress at $z=\bar{h}$ in eq (44), as described, could cause a reduction or vanishing in the calculated frictional turning of the wind with height at low levels.

An uncertainty in the prediction of $\bar{h}$ is whether it may become too large too frequently. Over land surfaces, the usual mechanism (included in sec. 5) that limits $\bar{h}$ is the occurrence of stable stratification at night. Over the sea, the main height limiting mechanism is similarly expected to be the eventual switch from equatorward movement of air, which had been receiving heat from the surface, to poleward movement over a cooler sea surface. Then the height limiting mechanism of stable stratification, eq (58), operates. Of course, the strong tendency for subsidence in equatorward moving air also limits $\bar{h}$ in cases with upward heat flux, as does the subsidence between cloud clusters over tropical waters. With these mechanisms included in section 5, it is believed that values of $\bar{h}$ calculated from eq (51) and (58) will be well behaved.

After completion of this study, the work by Clarke (1970*b*) on the same topic was pointed out to me. The two approaches are dissimilar in many respects, with the main differences being as follows:

1. Clarke does not attempt to calculate the stability-dependent and time-dependent height of the PBL. Instead, he recommends a PBL height that is a small fraction of 10 km in equatorial latitudes and of u_*/f elsewhere. Generally, he utilizes $|\mathbf{V}_1|/f$ in place of $\bar{h}$ where the latter appears in Ri_B and in $\bar{h}/z$, for determination of C_u and C_θ. As a result, it is difficult to compare results except to note that similar values for these coefficients using either method are obtained for the most frequently encountered conditions away from the Equator.

2. Clarke estimates the direction of the surface wind and stress with respect to the wind direction at level z_1. As a result, his surface wind does not necessarily have a component directed toward lower surface pressure as in this paper.

3. Clarke uses values from the lowest grid level of the GCM (his method II) as being representative of values at the top of the PBL, whereas here the *mean* values within the PBL are estimated with the aid of calculated values of $\bar{h}$.

4. In estimating the interior PBL fluxes for a GCM having very good vertical resolution at low levels, Clarke uses a mixing-length representation rather than scaled values based upon surface fluxes and $\bar{h}$ as in section 6.

The ideas presented in sections 3, 5, and 6 may be useful even if the GCM has such good vertical resolution that the angle of the surface wind need not be separately calculated. Prediction of the height of the PBL could be a great aid to forecasts of air pollution, in addition to being nearly essential if the turbulent transports initiated by the earth's surface are to be successfully parameterized.

ACKNOWLEDGMENTS

I thank A. Kasahara and A. Arakawa for independently suggesting the need for a comprehensive treatment of the planetary boundary layer and Y. Mintz for the invitation to spend 6 mo with the Department of Meteorology at UCLA where this study was undertaken. I appreciate the suggestions for manuscript improvement by Y. Mintz, A. Arakawa, D. Lilly, A. Kasahara, and W. Washington, and by W. Schubert of UCLA.

REFERENCES

Arakawa, Akio, Katayama, Akira, and Mintz, Yale, "Numerical Simulation of the General Circulation of the Atmosphere," *Proceedings of the WMO/IUGG Symposium on Numerical Weather Prediction, Tokyo, Japan, November 26–December 4, 1968*, Japan Meteorological Agency, Tokyo, Mar. **1969**, pp. IV–7—IV–8 and appendices.

Blackadar, Alfred K., and Tennekes, Hendrik, "Asymptotic Similarity in Neutral Barotropic Planetary Boundary Layers," *Journal of the Atmospheric Sciences*, Vol. 25, No. 6, Nov. **1968**, pp. 1015–1020.

Businger, Joost A., "Transfer of Momentum and Heat in the Planetary Boundary Layer," *Proceedings of the Symposium on the Arctic Heat Budget and Atmospheric Circulation, Lake Arrowhead, California, 1966, Research Memorandum* RM–5233–NSF, Rand Corporation, Santa Monica, Calif., Dec. **1966**, pp. 305–332.

Businger, Joost A., Wyngaard, John C., Izumi, Y., and Bradley, E. F., "Flux-Profile Relationships in the Atmospheric Surface Layer," *Journal of the Atmospheric Sciences*, Vol. 28, No. 2, Mar. **1971**, pp. 181–189.

Clarke, R. H., "Observational Studies in the Atmospheric Boundary Layer," *Quarterly Journal of the Royal Meteorological Society*, Vol. 96, No. 407, London, England, Jan. **1970***a*, pp. 91–114.

Clarke, R. H., "Recommended Methods for the Treatment of the Boundary Layer in Numerical Models," *Australian Meteorological Magazine*, Vol. 18, No. 2, Commonwealth Bureau of Meteorology, Melbourne, June **1970***b*, pp. 51–71.

Csanady, G. T., "On the 'Resistance Law' of a Turbulent Ekman Layer," *Journal of the Atmospheric Sciences*, Vol. 24, No. 5, Sept. **1967**, pp. 467–471.

Deardorff, James Warner, "A Three-Dimensional Numerical Investigation of the Idealized Planetary Boundary Layer," *Geophysical Fluid Dynamics*, Vol. 1, No. 4, Gordon & Breach Science Publishers, London, England, Nov. **1970***a*, pp. 377–410.

Deardorff, James Warner, "Preliminary Results From Numerical Integrations of the Unstable Planetary Boundary Layer," *Journal of the Atmospheric Sciences*, Vol. 27, No. 8, Nov. **1970***b*, pp. 1209–1211.

Deardorff, James Warner, "Convective Velocity and Temperature Scales for the Unstable Planetary Boundary Layer and for Rayleigh Convection," *Journal of the Atmospheric Sciences*, Vol. 27, No. 8, Nov. **1970***c*, pp. 1211–1213.

Deardorff, James Warner, "Numerical Investigation of Neutral and Unstable Planetary Boundary Layers," *Journal of the Atmospheric Sciences*, Vol. 28, No. 1, Jan. **1972**, pp. 91–115.

Deardorff, James Warner, Willis, Glen E., and Lilly, Douglas K., "Laboratory Investigation of Non-Steady Penetrative Convection," *Journal of Fluid Mechanics*, Vol. 35, Part 1, Cambridge University Press, London, England, Jan. **1969**, pp. 7–31.

455-016 O - 72 - 4

Dyer, A. J., "The Turbulent Transport of Heat and Water Vapor in an Unstable Atmosphere," *Quarterly Journal of the Royal Meteorological Society*, Vol. 93, No. 398, London, England, Oct. **1967**, pp. 501–508.

Fiedler, F. Munich, and Panofsky, Hans A., "The Geostrophic Drag Coefficient Over Heterogeneous Terrain," paper presented at the Second Canadian Conference on Micrometeorology, Macdonald College, Ste. Anne de Bellevue, Quebec, Canada, May 10–12, **1971**.

Fleagle, Robert G., Deardorff, James Warner, and Badgley, Frank I., "Vertical Distribution of Wind Speed, Temperature and Humidity Above a Water Surface," *Journal of Marine Research*, Vol. 17, Nov. **1958**, pp. 141–155.

Gill, Adrian E., "Similarity Theory and Geostrophic Adjustment," *Quarterly Journal of the Royal Meteorological Society*, Vol. 94, No. 402, London, England, Oct. **1968**, pp. 586–588.

Hasse, Lutz, "Zur Bestimmung der vertikalen Transporte von Impuls und fühlbarer Wärme in der wassernahen Luftschicht über See" (On the Determination of the Vertical Transports of Momentum and Heat in the Atmospheric Boundary Layer at Sea), *Hamburger Geophysikalische Einzelschriften* 11 (Hamburg Geophysical Monograph 11), Cram, deGruyter, Hamburg, Germany, **1968**, 70 pp.

Lavoie, Ronald L., Cotton, W. R., and Hovermale, John B., "Investigations of Lake-Effect Storms," *Final Report*, Contract No. E22–103–68(N), Department of Meteorology, The Pennsylvania State University, University Park, Jan. **1970**, 127 pp.

Lenschow, Donald H., "Airplane Measurements of Planetary Boundary Layer Structure," *Journal of Applied Meteorology*, Vol. 9, No. 6, Dec. **1970**, pp. 874–884.

Lenschow, Donald H., and Johnson, Warren B., Jr., "Concurrent Airplane and Balloon Measurements of Atmospheric Boundary-Layer Structure Over a Forest," *Journal of Applied Meteorology*, Vol. 7, No. 1, Feb. **1968**, pp. 79–89.

Leovy, Conway, and Mintz, Yale, "Numerical Simulation of the Atmospheric Circulation and Climate of Mars," *Journal of the Atmospheric Sciences*, Vol. 26, No. 6, Nov. **1969**, pp. 1167–1190.

Lettau, Heinz H., and Dabberdt, Walter F., "Variangular Wind Spirals," *Boundary-Layer Meteorology*, Vol. 1, No. 1, D. Reidel Publishing Co., Dordrecht, Holland, Mar. **1970**, pp. 64–79.

Lilly, Douglas K., "Models of Cloud-Topped Mixed Layers Under a Strong Inversion," *Quarterly Journal of the Royal Meteorological Society*, Vol. 94, No. 401, London, England, July **1968**, pp. 292–309.

Miyake, M., Donelan, M., McBean, G., Paulson, Clayton, Badgley, Frank I., and Leavitt, E., "Comparison of Turbulent Fluxes Over Water Determined by Profile and Eddy Correlation Techniques," *Quarterly Journal of the Royal Meteorological Society*, Vol. 96, No. 407, London, England, Jan. **1970**, pp. 132–137.

Panofsky, Hans A., "Determination of Stress From Wind and Temperature Measurements," *Quarterly Journal of the Royal Meteorological Society*, Vol. 89, No. 379, London, England, Jan. **1963**, pp. 85–94.

Paulson, Clayton A., "The Mathematical Representation of Wind Speed and Temperature Profiles in the Unstable Atmospheric Surface Layer," *Journal of Applied Meteorology*, Vol. 9, No. 6, Dec. **1970**, pp. 857–861.

Sheppard, Percival Albert, "Transfer Across the Earth's Surface and Through the Air Above," *Quarterly Journal of the Royal Meteorological Society*, Vol. 84, No. 361, London, England, July **1958**, pp. 205–224.

Smagorinsky, Joseph, "General Circulation Experiments With the Primitive Equations: I. The Basic Experiment," *Monthly Weather Review*, Vol. 91, No. 3, Mar. **1963**, pp. 99–164.

Smagorinsky, Joseph, Manabe, Syukuro, and Holloway, J. Leith, Jr., "Numerical Results From a Nine-Level General Circulation Model of the Atmosphere," *Monthly Weather Review*, Vol. 93, No. 12, Dec. **1965**, pp. 727–768.

Telford, James W., and Warner, J., "Fluxes of Heat and Vapor in the Lower Atmosphere Derived From Aircraft Observations," *Journal of the Atmospheric Sciences*, Vol. 21, No. 5, Sept. **1964**, pp. 539–548.

Tennekes, Hendrik, "Free Convection in the Turbulent Ekman Layer of the Atmosphere," *Journal of the Atmospheric Sciences*, Vol. 27, No. 7, Oct. **1970**, pp. 1027–1034.

Townsend, Allen A., "Natural Convection in Water Over an Ice Surface," *Quarterly Journal of the Royal Meteorological Society*, Vol. 90, No. 385, London, England, July **1964**, pp. 248–259.

Webb, E. K., "Profile Relationships: The Log-Linear Range and Extension to Strong Stability," *Quarterly Journal of the Royal Meteorological Society*, Vol. 96, No. 407, London, England, Jan. **1970**, pp. 67–90.

[*Received April 8, 1971; revised June 8, 1971*]